Journal of Radioanalytical and Nuclear Chemistry (2021) 327:1325–1333
https://doi.org/10.1007/s10967-021-07615-0

Enhancement of U(VI) biosorption by *Trichoderma harzianum* mutant obtained by a cold atmospheric plasma jet

Jun Liang[1] · Lei Liu[2] · Wencheng Song[2,3,4]

Received: 25 November 2020 / Accepted: 19 January 2021 / Published online: 15 February 2021

Abstract

Trichoderma harzianum (*T. harzianum*) was isolated from uranium mill tailing soils, and a cold atmospheric plasma jet as a mutational method was applied for the treatment of *T. harzianum* to improve its performance of U(VI) biosorption. The effects of pH, adsorption time and biosorbent doses were performed on the biosorption of U(VI) by *T. harzianum* and mutated *T. harzianum* at different environmental conditions. The maximum adsorbability for U(VI) on mutated *T. harzianum* was 83.59 mg/g at 303 K and pH 6.0, which was observably better than the raw *T. harzianum*. FTIR analysis indicated that the functional groups on the surface of mutated *T. harzianum* interacting with U(VI) were primarily hydroxyl, amino and carboxyl groups. SEM coupled with EDX analysis demonstrated that U(VI) can be adsorbed to mutated *T. harzianum*, and the surface of mutated *T. harzianum* became rough and incompact after the biosorption. This study showed that the mutated *T. harzianum* could be considered as a highly effective biosorbent for removal of U(VI) from radioactive wastewater.

Keywords Biosorption · *Trichoderma harzianum* · U(VI) · A cold atmospheric plasma jet

Introduction

Uranium, a scarce strategic resource in large demand, is massively exploited and widely used for nuclear power production [1]. However, with the development of the nuclear energy industries, large amounts of uranium-containing radioactivity wastewater were generated and leaked into adjacent soils and groundwater [2]. Due to the radioactivity and chemical toxicity of uranium, the free uranium(VI) (U(VI)) ions leaking into the environment will cause severe damage to human health and ecological environment [3]. Consequently, it is urgent to develop environment-friendly and efficient technologies to eliminate U(VI) from aqueous solution.

There are numerous treatment techniques for removing radionuclides from environment, including chemical precipitation, ion exchange, adsorption, extraction and so on [4–6]. Compared with traditional chemical treatment techniques, microbial bioremediation is gaining more and more attention, considering its high removal efficiency, low operation cost and no secondary pollution. Recent researches have revealed that different kinds of living microorganisms, such as bacteria [7, 8], fungi [9–11] and algae [12–14] have been used as biosorbents for binding U(VI) from aqueous solutions. Among them, filamentous fungi, such as *Rhizopus*, *Penicillium* and *Aspergillus*, have been proved to be promising biosorbents with favorable advantages for effective removal of uranium from radioactive wastewater [15–17]. In order to enhance the biosorption performance of microorganisms, various kinds of mutation strategies have been extensively applied [18–20]. Sun et al. used Hydroxylamine hydrochloride and UV light to mutate *Penicillium funiculosum*, and biosorption capacity of U(VI) on mutated *P. funiculosum* increased obviously [21]. Moreover, Song et al. employed dielectric barrier discharge plasma to alter

✉ Wencheng Song
wencsong@cmpt.ac.cn

1 School of Jianghuai, Anhui University, Hefei 230036, Anhui, People's Republic of China

2 Anhui Province Key Laboratory of Medical Physics and Technology, Institute of Health & Medical Technology, Hefei Institutes of Physical Science, Chinese Academy of Sciences, Hefei 230031, People's Republic of China

3 Hefei Cancer Hospital, Chinese Academy of Sciences, Hefei 230031, People's Republic of China

4 Collaborative Innovation Center of Radiation Medicine of Jiangsu Higher Education Institutions and School for Radiological and Interdisciplinary Sciences, Soochow University, Suzhou 215123, People's Republic of China

the DNA of *Aspergillus oryzae* for more effective mutants with improved bioremediation properties [22].

A cold atmospheric plasma jet (CAPJ) could produce reactive species, which is composed of an excited state of free radicals, ions, electrons, and reactive oxygen and nitrogen species [23]. In addition, CAPJ is a relatively soft ionization technology with higher ionization efficiency of low molecular weight compounds [24], and can induce DNA change in the cells, which indicates that CAPJ is an excellent technique to mutate microbes due to its high mutation rate, simple operation, low cost and shorter reaction time [25]. In fact, CAPJ has been successfully employed to mutate *Haematococcus pluvialis* [26], *Cladosporium sphaerospermum* [27], *Rhodosporidium toruloides* [20] and *Ganoderma lingzhi* [28].

In the present study, *T. harzianum* was isolated from the uranium mill tailing and its morphological characteristics were studied in details. In order to enhance U(VI) biosorption properties, CAPJ was conducted to mutate *T. harzianum* strain. Then, U(VI) biosorption characteristics of *T. harzianum* and mutated *T. harzianum* were invesigated in different environmental conditions, and possible biosorption mechanisms of mutated *T. harzianum* were explored by scanning electron microscopy (SEM) with Energy Dispersive X-Ray Spectroscopy (EDX), and Fourier Transform infrared spectroscopy (FTIR).

Materials and methods

Strain isolation and identification

The uranium contaminated soils were collected from a uranium mill tailing located in southern China, and the U(VI)-tolerance strains were isolated through standard dilution-plate method [29] in potato dextrose agar (PDA) plates which contained different concentrations of U(VI). The inoculated plates were incubated at 28 °C for 72 h. Then, the fungal isolates that could tolerate the highest U(VI) concentration were selected for purification and kept on fresh PDA plates. The pure fungal strain was identified by macroscopic characteristics using Olympus IX71 inverted fluorescence microscope (Olympus, Tokyo, Japan) and microscopic characteristics using molecular identification. Amplification of ITS region gene sequences was performed according to the previously method [30]. The purified product was followed by DNA sequencing (Sangon, Shanghai), and afterwards the sequence was analyzed with the BlastN search program in the NCBI GenBank database (http://blast.ncbi.nlm.nih.gov/). Then, the molecular phylogenetic analysis of the isolate was performed based on the ITS region gene sequence analysis.

Mutagenesis of the fungus

The CAPJ plasma for this work was schematically showed in Fig. 1a. The reactor chamber has 2 parallel copper electrodes with a distance of 60 mm. Helium (99.997% purity) gas was applied as the plasma working gas with its flow rate 900 mL/min, which was injected 2 min before the experiment to force air out from the reactor compartment. Spores of *T. harzianum* were collected from the mid-growth phase and diluted to 10^6–10^7/mL. Then the spore suspension was dripped onto sterilized plates and treated with CAPJ treatment for 3 min. After the CAPJ treatment, mutagenized spores were placed on the PDA solid medium and cultured for 3 days at 28 °C. Many survival single colonies with various morphologies were observed. Finaly, the high-growth-rate strain was selected and cultured for biosorption experiments.

Biomass preparation

Trichoderma harzianum and mutated *T. Harzianum* were used as adsorbents to remove U(VI) in this study. *T. harzianum* and mutated *T. Harzianum* were cultivated separately in the Erlenmeyer flasks (250 mL) containing 150 mL of PDA medium at 28 °C and agitated at 150 rpm. After 3 days of incubation, the fermentation broth was filtrated for the mycelia, and the mycelia was washed twice with distilled water and then freeze-dried for 24 h. Then, fungal biomass was stored separately in an amber bottle at a temperature of 4 °C until used for adsorption studies.

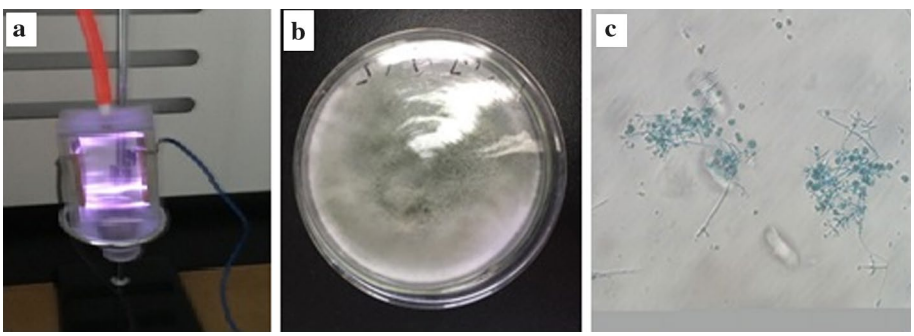

Fig. 1 The schematic of the plasma system and photograph of the reactor chamber (**a**); Colonies of the fungus grown on PDA solid medium for 5 days (**b**); Microscopic image of the fungus (laetophcnol cotton lalue dyeing) (**c**)

Characterization studies of biomass

The surface morphology and elemental composition of the mutated *T. harzianum* before and after loading of U(VI) were characterized by SEM coupled with EDX. For this purpose, The mycelia of mutated *T. harzianum* before and after loading of U(VI) were collected and washed three times with sterilized water. About 10 mg of the samples were solidified with 2.5% glutaraldehyde and then 1.0% osmic acid at room temperature for 1 h. After that, Samples were then dehydrated through a graded ethanol series, finally critical-point-dried, coated with gold and examined using a SEM (JEOL JSM-6330F, Japan) coupled with EDX (Oxford) system at 200 kV [31]. Infrared spectra of U(VI)-free and U(VI)-loaded mycelia prepared as KBr discs were recorded over the region 400–4000 cm^{-1} using a Perkin Elmer Spectrum 100 spectrophotometer (Waltham, MA, USA). Besides, The zeta potential of *T. harzianum* and mutated *T. harzianum* were investigated by an automatic titrator system (DL58, Mettler Toledo, Germany) at different pH values.

Biosorption experiments

In a general procedure, 0.05 g of uranium nitrate ($UO_2(NO_3)_2{\cdot}6H_2O$) was dissolved in 0.1 L deionized water to obtain a stock solution (500 mg/L). The stock solution was diluted to an appropriate concentration for experiments. All the biosorption experiments on *T. harzianum* and mutated *T. harzianum* were operated under ambient conditions. To investigate the influence of pH and concentrations of biosorbent on biosorption of U(VI) by *T. harzianum* and mutated *T. harzianum*, different conditions of pH (2–11) and concentrations of biosorbent (0.05–0.7 g/L) were performed by batch experiments. Afterwards, the suspensions were shocked at 150 rpm for 24 h to achieve biosorption equilibrium, and the solution was centrifuged at 8000 rpm for 10 min. The concentration of residual U(VI) was determined by a Packard 3100 TR/AB Liquid Scintillation Analyzer (Perkin-Elmer). All the experiments were conducted in triplicate. The removal efficiency (Removal, %) and Adsorption capacity (Q_e, mg/g) were determined by the following formulae:

$$\text{Removal}\,(\%) = \frac{C_0 - C_e}{C_0} \times 100\% \tag{1}$$

$$Q_e = \frac{C_0 - C_e}{m} \times V \tag{2}$$

where C_0 (mg/L) is the initial U(VI) concentration; C_e (mg/L) represents equilibrium U(VI) concentration; V (mL) is the volume of the suspension and m (g) is the weight of fungal mycelia.

Results and discussion

Strain identification

The fungal isolate showed similar features to *T. harzianum* species, such as rapid growth of colony, with dense conidiation, turning dark green after 5 days as shown in Fig. 1b, and abundant sporulation with spherical smooth conidia was arranged in clusters (Fig. 1c). Besides, the length of detected ITS gene sequence from the fungal isolate was approximately 591 bp, and phylogenetic relationships on the basis of ITS gene sequences were created in Fig. 2. The fungal isolate showed 99% sequence similarity to sequences of *T. harzianum* strain JZY4 (MT786378.1) and *T. harzianum* strain NZD-mf15 (KM278121.1). Combining with external morphological features and DNA identification, the fungal isolate was identified as *T. harzianum*.

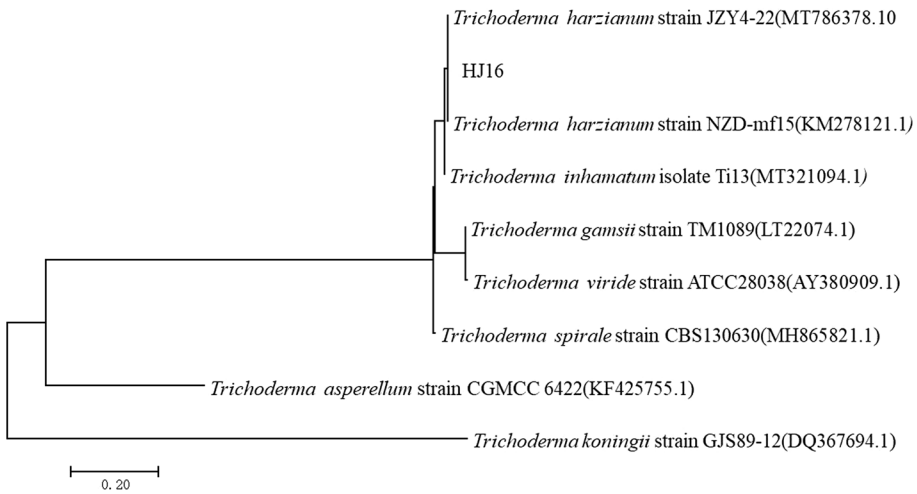

Fig. 2 Phylogenic tree based on fragments of ITS rRNA partial gene sequences

Effect of pH

The effect of the initial pH on the adsorption efficiency of U(VI) onto the *T. harzianum* and mutated *T. harzianum* biomass was presented in Fig. 3a. The adsorption rate increased obviously from pH 2.0 to 6.0, and achieved its maximum value at pH 6.0, above which it gradually reduced, which was consistent with the earlier study [32, 33]. From Fig. 3a, the highest removal efficiency of U(VI) onto mutated *T. harzianum* was about 90% at pH 6.0, which was approximately 10% more than that of *T. harzianum*. Earlier studies showed that modifications in pH could bring about changes in net charge of the mycelia surface but also changed the U(VI) species in the solution [34, 35]. The reason for this change trend of the adsorption rate may be due to a variation in the presence status of uranium. At low pH, uranium existed as the form of UO_2^{2+} in solution, and H^+ occupied the active binding sites thus the uranium removal efficiency was very low [36]. As pH value increased, the UO_2^{2+} gradually hydrolyzed to $(UO_2)_2(OH)_2^{2+}$, $(UO2)_3(OH)^{5+}$ and UO_2OH^+ [37], which bound more easily with active sites than H^+, and the mycelia surface carried with negative charges; therefore, the mycelia could adsorb more uranium ions [38]. However, when pH is over 6.0, hydrolyzed species of uranium and the zero point of charge (Fig. 5b) may lead to the decline of sorption efficiency of uranium [39, 40].

Effect of biosorbent dosage

The effect of biosorbent dosage on adsorption of U(VI) onto the *T. harzianum* and mutated *T. harzianum* adsorption was evaluated by varying biosorbent dosage from 0.05 g/L to 0.7 g/L (Fig. 3b). It showed that the removal efficiency of U(VI) increased from 42 to 85% and 50 to 88% for *T. harzianum* and mutated *T. harzianum*, respectively, when biomass dosage was increased from 0.05 to 0.5 g/L, while the distribution coefficient (Kd) for *T. harzianum* and mutated *T. harzianum* was decreased, respectively. This indicated that the number of the binding sites for uranium (VI) increased with the increase of the biosorbent dosage in the range of 0.05–0.5 g/L [41]. However, when the biosorbent dosage was more than 0.5 g/L, the biosorption rate of uranium (VI) from the solution was almost constant, and Kd for *T. harzianum* and *mutated T. harzianum* almost did not change. It may be attributed to the fact that higher biosorbent dosage could produce aggregation and competition among biosorbent particles, which reduces the effective binding sites of functional groups at the surface of mycelia [42]. Therefore, 0.5 g/L of biosorbent was used in subsequent U(VI) biosorption experiments.

Effect of adsorption time

Figure 4a revealed the effect of adsorption time on the biosorption of U(VI) onto the *T. harzianum* and mutated *T. harzianum* biomass. The rate of U(VI) adsorption on the *T. harzianum* and mutated *T. harzianum* biomass increased rapidly within 4 h, and then achieved dynamic sorption equilibrium at approximately 10 h, whereas the biosorption rate slightly became slow with the increase of adsorption time. The data of biosorption kinetics was analyzed using pseudo-first-order and pseudo-second-order kinetic. The calculation equations of these two kinetic models are given by Eqs. (3)–(4):

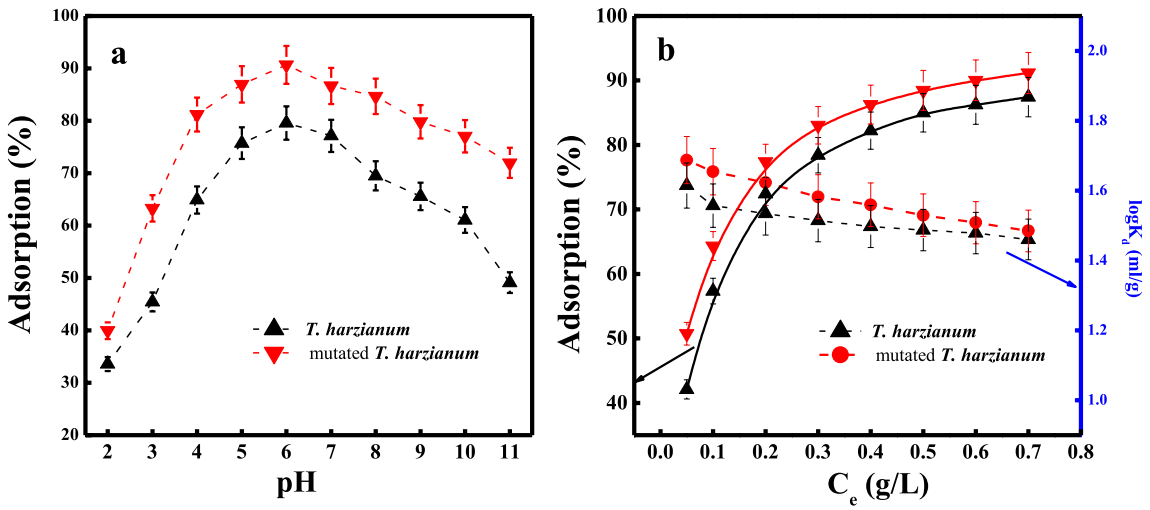

Fig. 3 Effect of pH on the adsorption of U(VI) by *T. harzianum* and mutated *T. harzianum* (**a**), $T = 303$ K, $m/V = 0.5$ g/L, $C_0 = 50$ mg/L; Effect of the biosorbent dosage on the adsorption of U(VI) by *T. harzianum* and mutated *T. harzianum*, $T = 303$ K, $C_0 = 50$ mg/L, pH = 6.0

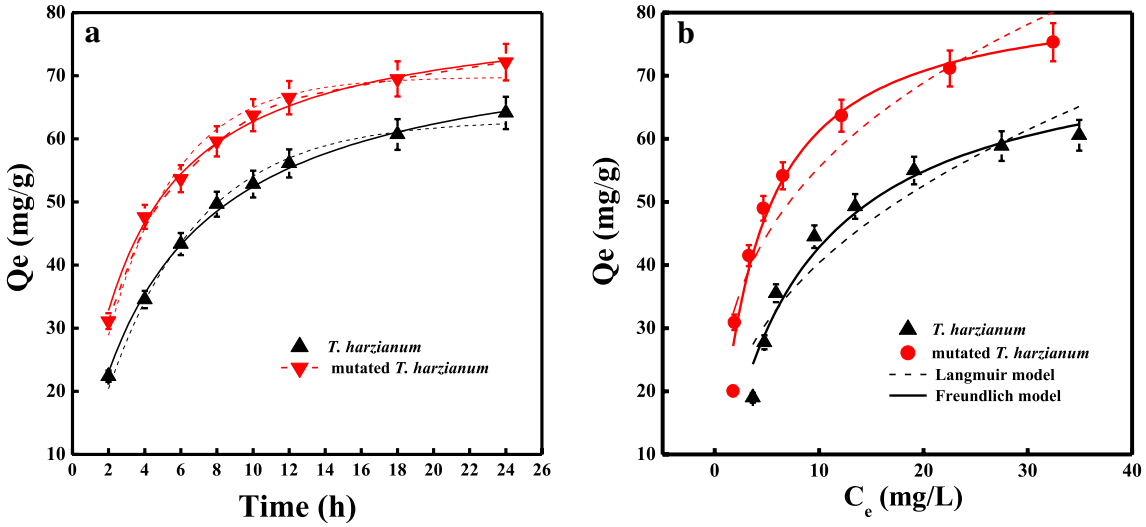

Fig. 4 Effect of adsorption time on U(VI) adsorption by *T. harzianum* and mutated *T. harzianum* (**a**), $T = 303$ K, $C_0 = 50$ mg/L, $m/V = 0.5$ g/L, pH = 6.0; The isotherms of U(VI) on *T. harzianum* and mutated *T. harzianum*, the solid line stands for Langmuir model and the dash line stands for Freundlich model (**b**), pH = 6.0, $m/V = 0.5$ g/L, $T = 303$ K

$$\ln(Q_e - Q_t) = \ln Q_e - \frac{k_1}{2.303}t \tag{3}$$

$$\frac{t}{Q_t} = \frac{1}{k_2 Q_e^2} + \frac{t}{Q_e} \tag{4}$$

where Q_t (mg/g) and Q_e represent the amounts of U(VI) adsorbed at time (t) and at equilibrium, respectively; k_1 (h^{-1}) and k_2 (g/(mg h)) are the adsorption rate constants of the pseudo-first-order and pseudo-second-order models, respectively. The fitting results and relevant parameters were listed in Table 1, respectively. Evidently, the biosorption kinetics of U(VI) on the *T. harzianum* and mutated *T. harzianum* were successfully described by the pseudo-second-order model ($R^2 > 0.999$), which indicated that the biosorption process was primarily controlled by chemical adsorption or ion exchange.

Adsorption isotherms

U(VI) adsorption isotherms of *T. harzianum* and mutated *T. harzianum* were shown in Fig. 4b. The amounts of U(VI) adsorption on *T. harzianum* and mutated *T. harzianum* enhanced dramatically with the increase of U(VI) concentration at pH 6.0 and 303 K. The experimental data of U(VI) adsorption were fitted with the Langmuir and Freundlich models to estimate the sorption capacity [43]. The calculation equations of these two isotherm models are as follows:

$$\frac{C_e}{Q_e} = \frac{1}{Q_m K_L} + \frac{C_e}{Q_m} \tag{5}$$

$$\ln Q_e = \ln K_F + \frac{1}{n}\ln C_e \tag{6}$$

where C_e (mg/L), the equilibrium concentration; Q_e (mg/g), the equilibrium biosorption capacity; Q_m (mg/g), the maximum monolayer adsorption capacity; K_L, K_F and n are the model constants of Freundlich and Langmuir, respectively.

The linearized form of Freundlich and Langmuir fitting isotherms were listed in Fig. 4b, and the calculated parameters were presented in Table 2. The Langmuir isotherm models of *T. harzianum* and mutated *T. harzianum* fitted better to the experimental data since their R^2 values were 0.989 and 0.993, respectively, which were higher than that of Freundlich model, suggesting that adsorption behavior of U(VI) onto *T. harzianum* and mutated *T. harzianum* cell surface may be a monolayer adsorption process. Similarly, uranium removal process by calcium alginate immobilized *Yarrowia lipolytica* powder beads

Table 1 The parameters of kinetic model for U(VI) adsoption by *T. harzianum* and mutated *T. harzianum*

Biosorbent	Pseudo-first-order			Pseudo-second-order		
	Q_e (mg/g)	k_1 (h^{-1})	R^2	Q_e (mg/g)	k_2 (g/(mg h))	R^2
T. harzianum	62.94	0.196	0.988	74.12	0.0034	0.999
Mutated *T. harzianum*	69.81	0.265	0.981	81.98	0.0042	0.999

was also shown to conform to Langmuir model [41]. As listed in Table 3, the maximum U(VI) sorption amount of mutated *T. harzianum* estimated from the Langmuir model was about 83.59 mg/g at 303 K and pH 6.0, which has higher Q_{max} for U(VI) sorption than other sorbents, such as *Rhodotorula glutinis* [34], *Streptomyces sporoverrucosus* [10], and immobilized *Aspergillus fumigatus* beads [14]. Therefore, mutated *T. harzianum* could be used as a promising biomaterial for removal of uranium from radioactive wastewater.

Biosorption mechanisms

In order to elucidate the active functional groups which participated in the mutated *T. harzianum* mycelia binding with uranium ions, FTIR spectra analyses were performed for control (U(VI)-free) and U(VI)-loaded mycelia between 4000 and 400 cm^{-1}. FTIR spectra of mutated *T. harzianum* without U(VI) and with U(VI) were presented in Fig. 5a. The results indicated that a distinct absorption peak at 3410–3460 cm^{-1} (O–H stretching vibration) was strengthened after adsorption, which indicated that –OH or –NH emerged on the mycelia surface combine with U(VI) ions through hydrogen binding [45, 46]. In addition, the peak at

Table 2 The parameters of Langmuir and Freundlich model for U(VI) adsoption by *T. harzianum* and mutated *T. harzianum*

Biosorbent	Langmuir model			Freundlich model		
	Q_m (mg/g)	K_L (L/mg)	R^2	K_F ((mg/g)/(mg L)$^{-n}$)	1/*n*	R^2
T. harzianum	75.24	0.128	0.989	16.714	0.383	0.902
Mutated *T. harzianum*	83.59	0.272	0.993	27.102	0.311	0.899

Table 3 Comparison of the maximum sorption capacities of U(VI) on various adsorbents

Sorbents	Experimental conditions		Q_{max} (mg/g)	Ref
	pH	*T* (K)		
Streptomyces sporoverrucosus dwc-3	3.0	303	2.07	[10]
Modified *Aspergillus nige*	5.0	298	6.789	[14]
Immobilized *Yarrowia lipolytica*	7.5	–	24.39	[41]
Immobilized *Rhodotorula glutinis*	6.0	298	27.69	[34]
Pseudomonas aeruginosa	5.0	293	44.1	[44]
Mutated *T. harzianum*	6.0	303	83.59	This study
Penicillium funiculosum	5.86	303	96.7	[21]

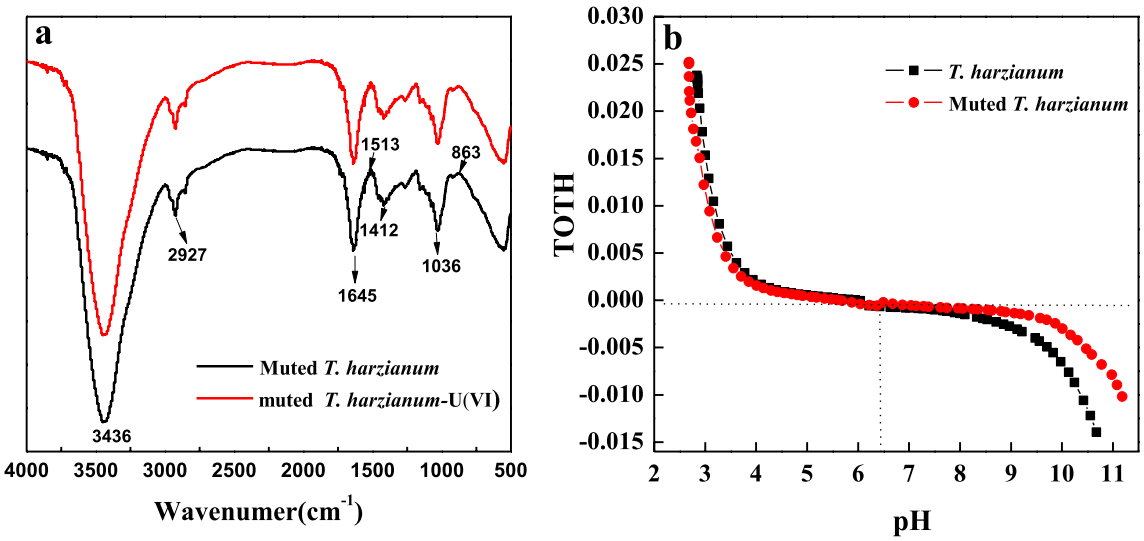

Fig. 5 FTIR spectra before and after U(VI) adsorption of mutated *T. harzianum* (**a**); zeta potential of *T. harzianum* and mutated *T. harzianum* (**b**)

2927 cm^{-1}, which may link with –CH asymmetric stretching vibrations, shifts to 2920 cm^{-1} after exposure to U(VI), indicating that the role of –CH groups in U(VI) binding. Moreover, The peaks at 1645 and 1432 cm^{-1} (C=O stretching vibration) also exhibit minor changes, which is possibly due to the complexing of the –C=O groups with U(VI) [47]. In summary, FTIR analysis revealed that the hydroxyl, amino and carboxyl groups of mutated *T. harzianum* cell wall played a significant role in the fungus U(VI) interaction.

SEM combined with EDX analyses was also used in order to understand mechanism of U(VI)-fungus interactions. The morphological change of mutated *T. harzianum* before (a), and after loading of U(VI) (b) were shown in Fig. 6. It can be seen that granular protrusions can be obviously observed on the SEM micrographs of the U(VI)-loaded mycelia as compared with the sample without loaded U(VI). The SEM images also demonstrated that U(VI)-loaded mutated *T. harzianum* changed their extracellular structure. On the basis of SEM observation, the place where there were attachments on the surface of the mycelium was selected for EDX analysis (the point indicated by the red arrow in Fig. 6c, d). The EDX chart originated from electron-dense bodies appeared the characteristic peak of uranium which ascertained the presence of U(VI) on the external surface of mutated *T. harzianum*, and carbon, phosphorus, oxygen and sodium were also found in the EDX chart. Therefore, it could be inferred that the surface of the mutated *T. harzianum* mycelium had a strong capacity to adsorb U(VI). Some literature reports also had shown similar mechanisms which the adsorbed U(VI) mainly occurred on the hyphal cell surfaces [17, 48]. Especially, the characteristic peak of phosphorus was found in EDX images, and it could be inferred that the precipitates of mycelium surface maybe a form of uranyl phosphates [49].

Based on the above analyses, the possible biosorption mechanism of U(VI) by mutated *T. harzianum* have been proposed. Firstly, U(VI) was attached on the hyphal cell surfaces. This behavior primarily due to the electrostatic interactions between U(VI) and high affinity sites of the fungal cell envelope. Meanwhile, The hyphal cell surfaces was covered with a lot of active functional groups, including hydroxyl, amino and carboxyl, which were also played a significant role in the fungus U(VI) interaction. Then under the stimulation of U(VI), the mutated *T. harzianum* released phosphate from cells by metabolism-dependent process. Therefore, U(VI) gradually form uranyl phosphates precipitates with released phosphate on the hyphal cell surfaces.

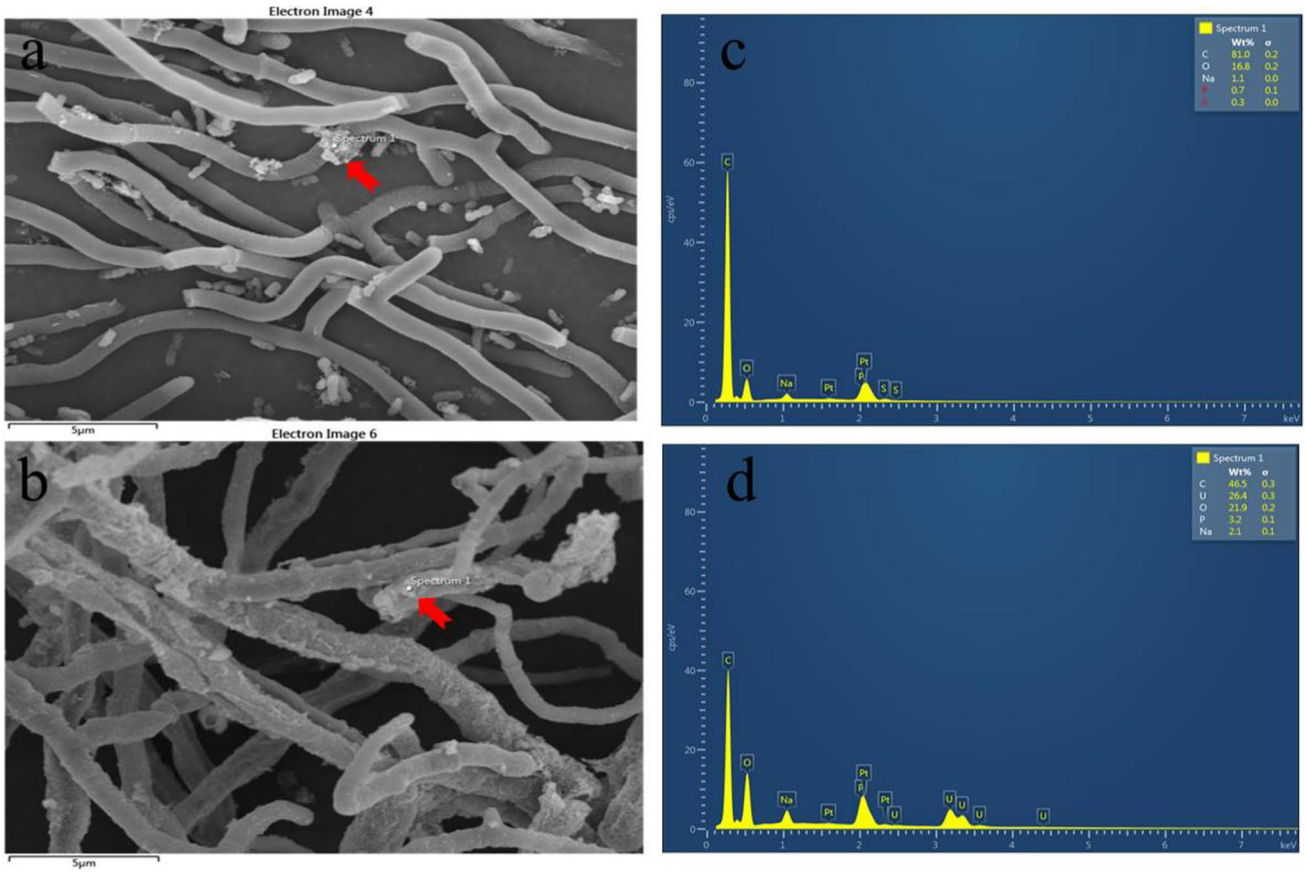

Fig. 6 SEM images and EDX spectra of selected area of mutated *T. harzianum* unloaded (**a**, **c**) and oaded with U(VI) (**b**, **d**)

However, the biosorption of U(VI) by *T. harzianum* is a complicated interaction process, and biosorption mechanism of U(VI) using *T. harzianum* and mutated *T. harzianum* still need to be further studied.

Conclusions

In this study, a resistant fungal strain for uranium adsorption was isolated from the uranium mill tailing soils. According to the morphology and the phylogenetic analysis based on ITS gene sequencing fragment (99% similarity to *T. harzianum*), it was identified synthetically as *T. harzianum*. *T. harzianum* was mutated by CAPJ to enhance U(VI) adsorption capacity. The mutated *T. harzianum* presented higher potential for U(VI) adsorption investigated by batch adsoption experiments. The experimental data better conformed to Langmuir model, and its maximum adsorbability for U(VI) was estimated to be 83.59 mg/g at pH 6.0 and 303 K. FTIR analysis indicated that U(VI) adhered to hydroxyl, amino and carboxyl groups in the mycelia cell wall of mutated *T. harzianum*. SEM coupled with EDX analysis demonstrated that U(VI) attached onto the surface of the mycelia. Therefore, the mutated *T. harzianum* could be considered as a highly effective sorbent for removal of uranium from radioactive wastewater.

Acknowledgements This research was supported by National Natural Science Foundation of China (22006001 and 21876179), the Key Project of Natural Scientific Research of Universities in Anhui Province (KJ2019A0914) and University Outstanding Young Scientific Research Talent Cultivation Program Project in Anhui Province (gxyq2020091).

References

1. Zhang YF, Zhu MY, Zhang S, Cai YW, Lv ZM, Fang M, Tan XL, Wang XK (2020) Highly efficient removal of U(VI) by the photoreduction of SnO_2/$CdCO_3$/CdS nanocomposite under visible light irradiation. Appl Catal B-Environ 279:119390
2. Szlachta M, Neitola R, Perniemi S, Vepslinen J (2020) Effective separation of uranium from mine process effluents using chitosan as a recyclable natural adsorbent. Sep Purif Technol 253:117493
3. Hund L, Bedrick EJ, Miller C, Huerta G, Nez T, Ramone S, Shuey C, Cajero M, Lewis J (2015) A Bayesian framework for estimating disease risk due to exposure to uranium mine and mill waste on the Navajo Nation. J R Stat Soc 178:1069–1091
4. Hamza MF, El-Aassy IE, Guibal E (2019) Integrated treatment of tailing material for the selective recovery of uranium, rare earth elements and heavy metals. Miner Eng 133:138–148
5. Rosenberg E, Pinson G, Tsosie R, Tutu H, Cukrowska E (2016) Uranium remediation by ion exchange and sorption methods: a critical review. Johnson Matthey Technol Rev 60:59–77
6. Liu P, Yu Q, Xue Y, Chen J, Ma F (2020) Adsorption performance of U(VI) by amidoxime-based activated carbon. J Radioanal Nucl Chem 324:813–822
7. Deng XY, Feng YL, Li HR, Yuan F, Teng Q, Wang HJ (2017) Adsorption properties of *Pseudomonas monteilii* for removal of uranium from aqueous solution. J Radioanal Nucl Chem 315:243–250
8. Sánchez-Castro I, Martínez-Rodríguez P, Jroundi F, Solari PL, Merroun ML (2020) High-efficient microbial immobilization of solved U(VI) by the *stenotrophomonas* strain Br 8. Water Res 183:116110
9. Bayramoglu G, Yakup Arica M (2016) Amidoxime functionalized *Trametes trogii* pellets for removal of uranium(VI) from aqueous medium. J Radioanal Nucl Chem 307:373–384
10. Li XL, Ding CC, Liao JL, Du L, Sun Q, Yang JJ, Yang YY, Zhang D, Tang J, Liu N (2016) Bioaccumulation characterization of uranium by a novel *Streptomyces sporoverrucosus* dwc-3. J Environ Sci 41:162–171
11. Bai J, Li Z, Fan FL, Wu XL, Tian W, Yin XJ, Zhao L, Fan FY, Tian LL, Wang Y, Qin Z, Guo JS (2014) Biosorption of uranium by immobilized cells of *Rhodotorula glutinis*. J Radioanal Nucl Chem 299:1517–1524
12. Ozudogru Y, Merdivan M (2020) Adsorption of U(VI) and Th(IV) ions removal from aqueous solutions by pretreatment with *Cystoseira barbata*. J Radioanal Nucl Chem 323:595–603
13. Erkaya IA, Arica MY, Akbulut A, Bayramoglu G (2014) Biosorption of uranium(VI) by free and entrapped *Chlamydomonas reinhardtii*: kinetic, equilibrium and thermodynamic studies. J Radioanal Nucl Chem 299:1993–2003
14. Bayramoglu G, Akbulut A, Arica MY (2015) Study of polyethyleneimine- and amidoxime-functionalized hybrid biomass of *Spirulina* (*Arthrospira*) *platensis* for adsorption of uranium (VI) ion. Environ Sci Pollut Res 22:17998–18010
15. Pang C, Liu YH, Cao XH, Li M, Huang GL, Hua R, Wang CX, Liu YT, An XF (2011) Biosorption of uranium(VI) from aqueous solution by dead fungal biomass of *Penicillium citrinum*. Chem Eng J 170:1–6
16. Wang JS, Hu XJ, Wang J, Bao ZL, Xie SB, Yang JH (2010) The tolerance of *Rhizopus arrihizus* to U(VI) and biosorption behavior of U(VI) onto *R. arrihizus*. Biochem Eng J 51:19–23
17. Ding HL, Zhang XN, Yang H, Zhang Y, Luo XG (2019) Biosorption of U(VI) by active and inactive *Aspergillus niger* equilibrium, kinetic, thermodynamic and mechanistic analyses. J Radioanal Nucl Chem 319:1261–1275
18. Bayramoglu G, Akbulut A, Acıkgoz-Erkaya I, Arica MY (2018) Uranium sorption by native and nitrilotriacetate-modified *Bangia atropurpurea* biomass: kinetics and thermodynamics. J Appl Phycol 30:649–661
19. Li XY, Liu RJ, Li J, Chang M, Liu YF, Jin QZ, Wang XG (2015) Enhanced arachidonic acid production from *Mortierella alpina* combining atmospheric and room temperature plasma (ARTP) and diethyl sulfate treatments. Bioresour Technol 177:134–140
20. Qi F, Kitahara Y, Wang Z, Zhao X, Du W, Liu D (2014) Novel mutant strains of *Rhodosporidium toruloides* by plasma mutagenesis approach and their tolerance for inhibitors in lignocellulosic hydrolyzate. J Chem Technol Biotechnol 89:735–742
21. Sun J, Li Q, Wang YD, Zhou ZX, Ding DX (2015) Isolation of a strain of *Penicillium funiculosum* and mutational improvement for UO_2^{2+} adsorption. J Radioanal Nucl Chem 303:427–432
22. Song WC, Wang XX, Wen T, Wang HQ, Hayat T, Wang XK (2016) Enhanced accumulation of U(VI) by *Aspergillus oryzae* mutant generated by dielectric barrier discharge air plasma. J Radioanal Nucl Chem 310:1353–1360
23. Lopez M, Calvo T, Prieto M, Mugica-Vidal R, Muro-Fraguas I, Alba-Elias F, Alvarez-Ordonez A (2019) A review on non-thermal atmospheric plasma for food preservation: mode of action, determinants of effectiveness, and applications. Front Microbiol 10:622
24. Wang XC, Hua ZD, Yang ZG, Li HP, Nie HG (2018) Low temperature plasma probe mass spectrometry based method for new psychoactive substances determination in oral fluid. Rapid Commun Mass Spectrom 32:11

25. Wang DD, Zou YQ, Tao L, Zhang YQ, Liu ZJ, Du SQ, Zang SQ, Wang SY (2019) Low-temperature plasma technology for electrocatalysis. Chin Chem Lett 30:826
26. Chen Z, Chen J, Liu JH, Li LM, Qin S, Huang Q (2020) Transcriptomic and metabolic analysis of an astaxanthin-hyperproducing *Haematococcus pluvialis* mutant obtained by low-temperature plasma (LTP) mutagenesis under high light irradiation. Algal Res 45:101746
27. Liang J, Li LM, Song WC (2018) Improved Eu(III) immobilization by *Cladosporium sphaerospermum* induced by low-temperature plasma. J Radioanal Nucl Chem 316:963–970
28. Ma YH, Zhang QQ, Zhang QF, He HQ, Chen Z, Zhao Y, Wei D, Kong MG, Huang Q, Metsälä M (2018) Improved production of polysaccharides in *Ganoderma lingzhi* mycelia by plasma mutagenesis and rapid screening of mutated strains through infrared spectroscopy. PLoS ONE 13:e0204266
29. Song WC, Liang J, Wen T, Wang XX, Hu J, Hayat T, Alsaedi A, Wang XK (2016) Accumulation of Co(II) and Eu(III) by the mycelia of *Aspergillus Niger* isolated from radionuclide-contaminated soils. Chem Eng J 304:186–193
30. Han GM, Feng XG, Jia Y, Wang CY, He XB, Zhou QY, Tian XG (2011) Isolation and evaluation of terrestrial fungi with algicidal ability from Zijin Mountain, Nanjing, China. J Microbiol 49:562–567
31. El-Sayed MT (2015) An investigation on tolerance and biosorption potential of *Aspergillus awamori* ZU JQ 965830.1 to Cd(II). Ann Microbiol 65:69–83
32. Bai J, Yao HJ, Fan FL, Lin MS, Zhang LN, Ding HJ, Lei F, Wu XL, Li XF, Guo JS, Qin Z (2010) Biosorption of uranium by chemically modified *Rhodotorula glutinis*. J Environ Radioact 101:969–973
33. Bai J, Wu XL, Fan FL, Tian W, Yin XJ, Zhao L, Fan FY, Li Z, Tian LL, Qin Z, Guo JS (2012) Biosorption of uranium by magnetically modified *Rhodotorula glutinis*. Enzyme Microb Technol 51:382–387
34. Altıntıg E, Altundag H, Tuzen M, Sarı A (2017) Effective removal of methylene blue from aqueous solutions using magnetic loaded activated carbon as novel adsorbent. Chem Eng Res Des 122:151–163
35. Cao Q, Liu Y, Wang C, Cheng J (2013) Phosphorus-modified poly (styrene-co-divinylbenzene)-PAMAM chelating resin for the adsorption of uranium(VI) in aqueous. J Hazard Mater 263:311–321
36. Leyva-Ramos R, Bernal-Jacome LA, Acosta-Rodriguez I (2005) Adsorption of cadmium(II) from aqueous solution on natural and oxidized corncob. Sep Purif Technol 45(1):41–49
37. Khani MH, Keshtkar AR, Meysami B, Zarea MF, Jalali R (2006) Biosorption of uranium from aqueous solution by nonliving biomass of marine algae *Cystoseira ndica*. Electron J Biotechnol 9(2):100–106
38. Chen F, Tan N, Long W, Yang SK, She ZG, Lin CY (2014) Enhancement of uranium(VI) biosorption by chemically modified marine-derived mangrove endophytic fungus *Fusarium* sp. #ZZF51. J Radioanal Nucl Chem 299:193–201
39. Zhu W, Liu Z, Chen L, Dong Y (2011) Sorption of uranium(VI) on Na-attapulgite as a function of contact time, solid content, pH, ionic strength, temperature and humic acid. J Radioanal Nucl Chem 289(3):781–788
40. Bursali EA, Merdivan M, Yurdakoc M (2009) Preconcentration of uranium(VI) and thorium(IV) from aqueous solutions using low-cost abundantly available sorbent: sorption behaviour of uranium(VI) and thorium(IV) on low-cost abundantly available sorbent. J Radioanal Nucl Chem 283(2):471–476
41. Kolhe N, Zinjarde S, Acharya C (2020) Removal of uranium by immobilized biomass of a tropical marine yeast *Yarrowia lipolytica*. J Environ Radioact 223–224:106419
42. Li L, Hu N, Ding DX, Xin X, Wang YD, Xue JH, Zhang H, Tan Y (2015) Adsorption and recovery of U(VI) from low concentration uranium solution by amidoxime modified *Aspergillus niger*. RSC Adv 5(81):65827–65839
43. Saleh TA, Sar A, Tuzen M (2017) Effective adsorption of antimony(III) from aqueous solutions by polyamide- graphene composite as a novel adsorbent. Chem Eng J 307:230–238
44. Texier AC, Andres Y, Cloirec PL (1999) Selective biosorption of lanthanide (La, Eu, Yb) ions by *Pseudomonas aeruginosa*. Environ Sci Technol 33:489–4954
45. Huang FY, Zhang HL, Wang YP, Yi FC, Huang HX, Cheng MX, Cheng J, Yuan WJ, Zhang J (2020) Uranium speciation and distribution in *Shewanella putrefaciens* and anaerobic granular sludge in the uranium immobilization process. J Radioanal Nucl Chem 326:393–405
46. Kushwaha S, Sreedhar B, Padmaja P (2012) XPS, EXAFS, and FTIR as tools to probe the unexpected adsorption-coupled reduction of U(VI) to U(V) and U(IV) on *Borassus flabellifer*-based adsorbents. Langmuir 28:16038–16048
47. Kazy SK, D'Souza SF, Sar P (2009) Uranium and thorium sequestration by a *Pseudomonas* sp.: mechanism and chemical characterization. J Hazard Mater 163:65–72
48. Coelho E, Reis TA, Cotrim M, Mullan TK, Corrêa B (2020) Resistant fungi isolated from contaminated uranium mine in Brazil shows a high capacity to uptake uranium from water. Chemosphere 248:126068
49. Wang TS, Zheng XY, Wang XY, Lu X, Shen YH (2017) Different biosorption mechanisms of uranium(VI) by live and heat-killed *saccharomyces cerevisiae* under environmentally relevant conditions. J Environ Radioact 167:92–99